

15. Coherence Transfer

In introducing coherence transfer, it is easy to get bogged down in a large number of product operator terms and obscure terminology. Here I present a simplistic approach to coherence transfer. I apologize to those who don't like semi-classical, hand-waving descriptions of quantum mechanics. The experiment I will use here to introduce the subject is an old experiment that has little direct practicality in modern multidimensional NMR. However, it serves as an important "building block" in many multidimensional heteronuclear experiments. The experiment correlates the chemical shifts of a proton and its attached carbon by transferring frequency labeled proton magnetization to a directly bonded carbon and detecting the carbon signal. Variants of this experiment are very important in many current multidimensional, heteronuclear experiments.

15.1 INEPT Type Transfer¹

The one-bond coupling constant between a ^1H and ^{13}C , $^1J_{\text{HC}}$, is about 140 Hz for aliphatic (sp^3) type carbons. The semiclassical picture of an ensemble of ^1H nuclei attached to ^{13}C nuclei is a mixture of molecules with about half of the protons attached to a ^{13}C nucleus with spin "down," β , and the remainder attached to nuclei with spin "up", α . The attached α and β ^{13}C nuclei give rise to different local magnetic fields at the ^1H nucleus. One ^{13}C spin state adds to the external magnetic field and increases the frequency of resonance, while the other state decreases the magnetic field and the corresponding resonance frequency. The one dimensional ^1H NMR spectrum of a molecule containing a ^1H attached to a ^{13}C (such as $^{13}\text{C}^1\text{HCl}_3$ ignoring the quadrupolar spins on the Cl nucleus) consists of a doublet centered at the ^1H frequency and split by the frequency of the coupling constant J_{HC} . The two peaks arise from the α -labeled ^1H and the β -labeled ^1H ,

$$\langle\alpha\rangle[-\text{H}_y] + \langle\beta\rangle[-\text{H}_y] \quad (15.1.1)$$

where the $\langle\alpha\rangle$ and $\langle\beta\rangle$ can be viewed as weighting coefficients having values determined from the ^{13}C Boltzmann distribution.

Upon applying a 90° pulse to the mixture of longitudinal ^1H spins with polarization ϵ at thermal equilibrium (Figure 15.1.1), we have,

$$\epsilon\{\langle\alpha\rangle\text{H}_z + \langle\beta\rangle\text{H}_z\} \xrightarrow{\pi/2\hat{H}_x} \epsilon\{\langle\alpha\rangle[-\text{H}_y] + \langle\beta\rangle[-\text{H}_y]\} \quad (15.1.2)$$

The amplitude of the induced transverse magnetization is ϵ . If the proton resonance, in the absence of coupling, is on-resonance (i.e. zero frequency in the rotating frame), then the two \mathbf{H}_y vectors will precess in opposite directions, each precessing away from

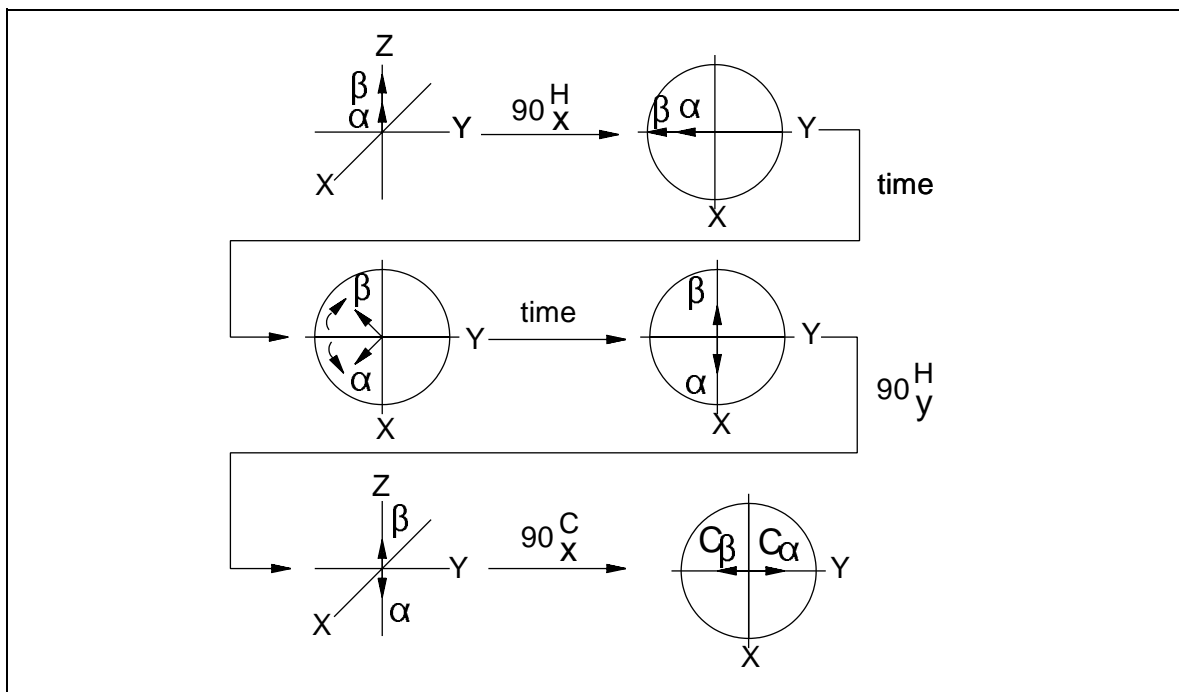


Figure 15.1.1. Vector representation of INEPT transfer for a coupled ^1H - ^{13}C spin system.

the $-Y$ axis due to the local magnetic fields generated by the opposite spin states of the attached ^{13}C nucleus. The frequency difference between the two vectors is equal to the coupling constant. At a time equal to $[1/(2 \cdot J_{\text{CH}})]$, the two spin vectors will have precessed into opposite positions along the X coordinate axis.

$$\epsilon\{\langle\alpha\rangle[-\mathbf{H}_y] + \langle\beta\rangle[-\mathbf{H}_y]\} \xrightarrow{1/(2 \cdot J_{\text{CH}})} \epsilon\{\langle\alpha\rangle[\mathbf{H}_x] + \langle\beta\rangle[-\mathbf{H}_x]\} \quad (15.1.3)$$

Eqn. 15.1.3 can be rearranged to

$$\epsilon\{\langle\alpha\rangle\mathbf{H}_x - \langle\beta\rangle\mathbf{H}_x\} = \epsilon\{\mathbf{H}_x(\langle\alpha\rangle - \langle\beta\rangle)\}, \quad (15.1.4)$$

but the quantity $(\langle\alpha\rangle - \langle\beta\rangle)$ is proportional to the longitudinal magnetization of the coupled spin \mathbf{C}_z .² By substituting \mathbf{C}_z for $(\langle\alpha\rangle - \langle\beta\rangle)$ one obtains

$$\epsilon\{\mathbf{H}_y\} \xrightarrow{1/(2 \cdot J_{\text{CH}})} \{2\mathbf{H}_x\mathbf{C}_z\} \quad (15.1.5)$$

where the "2" preceding the operator is a normalization factor. The state $2\mathbf{H}_x\mathbf{C}_z$ is an

antiphase state; \mathbf{H}_x magnetization is antiphase with respect to \mathbf{C} . As evolution of the spins continues, the two proton vectors align along the \mathbf{H}_y axis at time $1/J_{CH}$, then after a total period of $3/(2J_{CH})$ the antiphase state $-\mathbf{2H}_x\mathbf{C}_z$ will form, and finally $-\mathbf{H}_y$ will return at a total time of $2/(J_{CH})$. The time dependence is represented as

$$-\mathbf{H}_y = \pi J_{CH} t \hat{H}_z \hat{C}_z \Rightarrow -\mathbf{H}_y \cos(\pi J_{CH} t) + \mathbf{2H}_x\mathbf{C}_z \sin(\pi J_{CH} t). \quad (15.1.6)$$

Transverse magnetization oscillates between inphase, $-\mathbf{H}_y$, and antiphase magnetization, $\mathbf{2C}_z\mathbf{H}_x$. Note that the rotation operator is $\pi J_{CH} t \hat{H}_z \hat{C}_z$ for the coupling interaction.

If the spin system is in the $\mathbf{2H}_x\mathbf{C}_z$ state and a 90_y° pulse is applied to the ^1H nuclei, rotates the antiphase vectors into the $\pm Z$ axis (Figure 15.1.1). This is described in product operators as the single state of longitudinal two-spin order, $\mathbf{2H}_z\mathbf{C}_z$.

$$\epsilon\{\mathbf{2H}_x\mathbf{C}_z\} = \pi/2 \hat{H}_y \Rightarrow \epsilon\{\mathbf{2H}_z\mathbf{C}_z\} \quad (15.1.7)$$

Semi-classically, one vector can be associated with a Boltzmann equilibrium population while the other has an inverted population. To better visualize this process, Figure 15.1.2 shows the energy level diagrams for a two-spin $^1\text{H}-^{13}\text{C}$ spin system in various polarization states. Schematic one-dimensional spectra in each panel of Figure 15.1.2

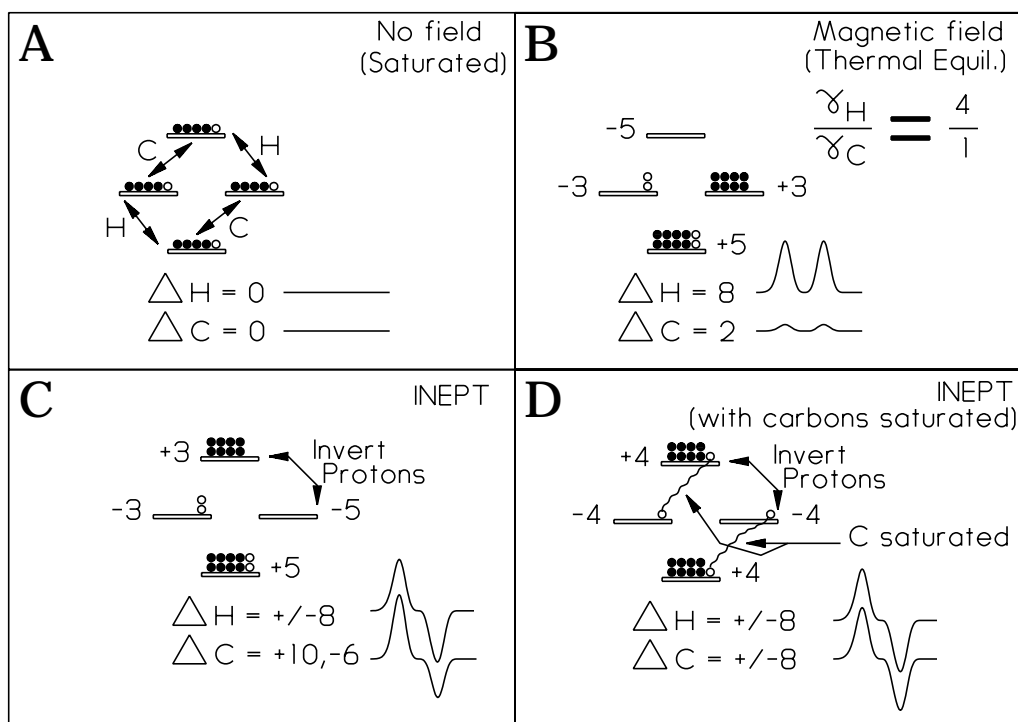


Figure 15.1.2. Energy level diagrams of a two-spin $^1\text{H}-^{13}\text{C}$ system showing various polarizations.

represent the signals that would be obtained by applying a 90° pulse to the various polarization states. Figure 15.1.2A is the energy level diagram for the system that has just had the magnetic field applied. The energy levels have been established, but there has not been time to establish thermal equilibrium. In Figure 15.1.2B, the system has reached Boltzmann equilibrium through the processes of spin-lattice relaxation. The polarization across the ¹H transitions is four times that of the ¹³C spins, reflecting the 4:1 ratio of the ¹H magneticogyric ratio to that of ¹³C. Panel C of Figure 15.1.2 represents a state in which the ¹H spin polarization across one transition has been inverted. A spectrum of the ¹H spins would show one peak of the doublet inverted with respect to the other. Since the ¹³C spins share the same energy levels, the population differences across the ¹³C transitions are also perturbed. In Figure 15.1.2D, where the ¹³C spins are saturated, the polarization across the ¹³C transitions is identical to those across the ¹H transitions. If a 90° pulse is applied to the ¹³C spins in the states described in Figure 15.1.2C or Figure 15.1.2D, the transverse ¹³C coherence, which is antiphase to ¹H, reflects the perturbed populations. A comparison of Figure 15.1.2B with Figure 15.1.2C and Figure 15.1.2D, shows the increased signal amplitude of the ¹³C spins due to polarization transfer from the ¹H spins.

$$\epsilon\{2H_z C_z\} = \pi/2 \hat{C}_x \Rightarrow \epsilon\{-2H_z C_y\} \quad (15.1.8)$$

Like the antiphase ¹H coherence, this coherence evolves due to scalar coupling into an inphase ¹³C resonance in a time of 1/(2J_{CH}).

$$\epsilon\{-2H_z C_y\} = \pi J_{CH} (1/(2J_{CH}) 2\hat{H}_z \hat{C}_z \Rightarrow \epsilon\{C_x\} \quad (15.1.9)$$

The initial polarization of the ¹H spins, ϵ , has been transferred to the ¹³C spins by this sequence (Eqn. 15.1.9).

As in the EXSY experiment, the ¹H spins can be frequency labeled by point-by-point sampling of a t_1 evolution period during which the ¹H spins precess under the chemical shift Hamiltonian. The chemical shift is represented as a modulation of the transferred polarization and in turn a signal amplitude of the ¹³C spins. The amplitude modulation of the ¹³C spins encodes the ¹H chemical shift frequency obtained during the t_1 period.

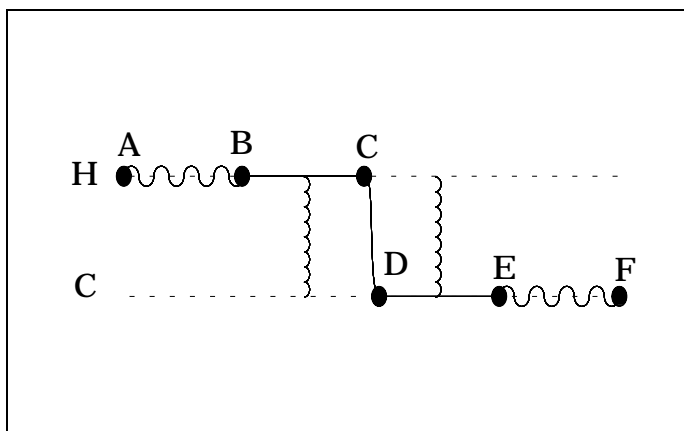


Figure 15.1.3. CFN for a ¹³C{¹H} chemical shift correlation experiment.

One can now design a 2D

experiment using this mechanism of coherence transfer. Without detailing the exact pulse sequence, this experiment can be described with a coherence flow network (CFN). The CFN for this experiment is shown in Figure 15.1.3. The letters in brackets, *e.g.* <A,B>, correspond to the various sections of the CFN. The spins are assumed to be in thermal equilibrium at state <A>. A 90° pulse transfers the ^1H magnetization into the transverse plane. The section <A,B> represents the chemical shift precession of the ^1H spins, this is the t_1 period that will be sampled point-by-point in time. The absence of any modifier during this period shows that the chemical shift precession is not modulated by any coupling, *i.e.* the carbons are decoupled from the protons. At state B, the ^1H spins have been frequency labeled. During the <B,C> period, active coupling (Table 1.1A) between ^1H and ^{13}C evolves without any chemical shift precession (Table 1.1T). At state <C>, the proton spin is antiphase with respect to the carbon spin. Coherence transfer from transverse ^1H to transverse ^{13}C occurs along <C,D>. Active coupling between the spins evolves during <D,E> refocusing the antiphase state at <D> to an inphase ^{13}C spin at <E>. The total period <B,E> represents a refocused INEPT transfer. Finally, the chemical shift frequency of the ^{13}C spin without coupling to ^1H is detected during <E,F>. Two-dimensional Fourier transform of the resulting $S(t_1, t_2)$ data yields a spectrum with a peak arising at the chemical shift coordinates of the ^1H and its coupled ^{13}C . Figure 15.1.4 is a schematic 2D $^{13}\text{C}\{^1\text{H}\}$ spectrum that might be collected using an experiment of this type. Along the top of Figure 15.1.4 is the (schematic) 1D ^{13}C spectrum and along the side is the corresponding 1D ^1H spectrum. At the intersection of pairs of ^1H - ^{13}C frequencies are cross peaks establishing that the two nuclei are directly coupled.

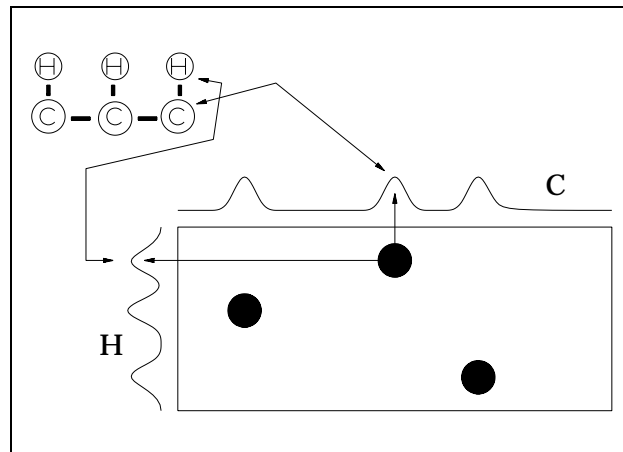


Figure 15.1.4. Schematic $^{13}\text{C}\{^1\text{H}\}$ heteronuclear chemical shift correlation spectrum.

1. G. Morris and R. Freeman (1979) *J. Am. Chem. Soc.* **101**, 760.
2. R. M. Lynden-Bell, J. M. Bulsing, and D. M. Doddrell (1983) *J. Magn. Reson.* **55**, 128.